Theoretical model of 180° domain-wall structures and their transformation in ferroelectric perovskites

X. R. Huang, X. B. Hu, S. S. Jiang, and D. Feng
National Laboratory of Solid State Microstructures and Department of Physics, Nanjing University, Nanjing 210093, People's Republic of China
(Received 26 June 1996)

Two kinds of 180° domain wall structures in the tetragonal phase of ferroelectric perovskites, one of the ''Ising type'' with only one polarization component and the other of the ''Bloch type'' with two polarization components within the wall layer, have been derived from the Landau-Ginzburg phenomenological theory. Temperature dependence of the interfacial energy indicates that the 180° wall has its own ''structural transformation,'' i.e., the wall structure is possible to change from Ising type to Bloch type upon cooling. As a more stable structure than the Ising-type wall in a wide temperature region, the Bloch-type wall has special crystal symmetry and physical properties which are presented in the report. [S0163-1829(97)07801-6]

The 180° domain walls separating domains with opposing spontaneous polarization can occur in all ferroelectrics, and their structure and energy play very important roles in the domain formation, configuration, and switching.[1] Due to their finite thickness, domain walls are usually difficult to be observed and measured directly by conventional techniques. Although high-resolution transmission electron microscopy can sometimes be used to reveal the atomic structures of domain walls,[2] it is questionable whether the structures observed in thin films may represent the real interfaces in bulk crystals (since ferroelectric films have strong surface effect). Thus, understanding of domain wall structures from experiments remains one of the prime tasks in the study of ferroelectricity and ferroelectric phase transitions. In theory, however, the Landau-Ginzburg phenomenological model has been applied successfully to describe the structural aspects of domain walls on the basis of a series of macroscopic physical quantities.[3–7] In the framework of this theory, the polarization profile of 180° walls is often described by a kink-type solitary-wave solution, and the wall properties associated with this solution, such as the thermal broadening and energy variation, can be verified directly or indirectly from experiments for certain ferroic systems.[8–11]

Many important ferroelectric materials have the perovskite structure, in which the 180° walls are critical to the performance of the related devices. Unlike that of uniaxial ferroelectrics, the spontaneous polarization vector of perovskites can take more than one component along the three $\langle 100 \rangle$ directions of the prototypic cubic structure,[12] which makes the wall structure much complicated. In this report, we demonstrate that, besides the conventional kink solution of the one-component polarization profile which has been presented in the previous works,[4,8] the 180° wall in perovskites has another kind of structure whose polarization is represented by two position-dependent components. Moreover, it seems that other kinds of domain walls in perovskites may also have the two-component-like solutions for the polarization configurations. Investigation of such kinds of walls can provide new insights into the mechanisms of domain dynamics and ferroelectric phase transitions.

The Helmholtz free-energy density for the centrosymmetric cubic perovskite structure is

$$F(P_i, P_{i,j}, \eta_{kl}) = F_P(P_i) + F_{\rm el}(\eta_{kl}) + F_c(P_i, \eta_{kl}) + F_G(P_{i,j}), \tag{1}$$

where F_P and $F_{\rm el}$ are Taylor series expansions in powers of the spontaneous polarization $\mathbf{P}=(P_1,P_2,P_3)$ and the elastic strain $\{\eta_{kl}\}$ $(k,l=1,2,3)$, respectively, F_c is the coupling energy between $\mathbf{P}$ and $\{\eta_{kl}\}$, and F_G is the gradient energy corresponding to the spatially inhomogeneous configuration of $\mathbf{P}$ within the domain wall layer (see Refs. 8 and 12). At zero external force, one has $\sigma_{ij}=(\partial F/\partial \eta_{kl})_{T,P}=0$, or

$$\eta_{ii} = Q_{11}P_i^2 + Q_{12}(P_j^2+P_k^2) \quad (i\neq j\neq k),$$
$$\eta_{ij} = Q_{44}P_iP_j \quad (i\neq j), \tag{2}$$

where the σ_{ij} are the Cauchy stress components and the Q_{ij} are determined by the elastic constants C_{ij} and the electrostrictive constants q_{ij}.[12] Based on Eq. (2), the total free energy of the homogeneous state can be rewritten as

$$F = \alpha_1 \sum_i P_i^2 + \alpha'_{11} \sum_i P_i^4 + \alpha'_{12} \sum_{i<j} P_i^2P_j^2 + \alpha_{111} \sum_i P_i^6 + \alpha_{112} \sum_{i\neq j} P_i^4P_j^2 + \alpha_{123}P_1^2P_2^2P_3^2. \tag{3}$$

Here $F_{\rm el}$ and F_c are included in the fourth power terms of Eq. (3). In the homogeneous tetragonal phase with the tetragonal axis parallel to x_1, the polarization has the form $(P_0,0,0)$ with

$$P_0 = \left(\frac{-\alpha'_{11} + \sqrt{{\alpha'_{11}}^2 - 3\alpha_1\alpha_{111}}}{3\alpha_{111}} \right)^{1/2}. \tag{4}$$

For a (001) 180° domain wall in a tetragonal perovskite with boundary conditions

$$\lim_{x_3\to\pm\infty} P_1 = \pm P_0, \qquad \lim_{x_3\to\pm\infty} P_2 = 0, \tag{5}$$

we can assume that $\mathbf{P}$ and η_{ij} vary only along x_3 in the bulk (neglecting the edge effect). Due to the nonzero conductivity of real ferroelectric perovskites, $\nabla\cdot\mathbf{P}=0$ gives $P_3\equiv 0$. Thus the polarization vector within the wall layer has the form $(P_1,P_2,0)$. The compatibility relations of the strain components[13] require $\eta_{11}\equiv Q_{11}P_0^2$, $\eta_{22}\equiv Q_{12}P_0^2$, and $\eta_{12}\equiv 0$ across the wall. For the stress components σ_{ij}, the equilibrium wall requires $\Sigma_j\sigma_{ij,j}=0$, which leads to $\eta_{13}=\eta_{23}=0$ and

$$\eta_{33}=\frac{q_{11}}{C_{11}}(P_1^2+P_2^2)-\frac{C_{12}}{C_{11}}(Q_{11}+Q_{12})P_0^2. \tag{6}$$

In view of the relations between η_{ij} and P_i, the free energy in the wall region can be reexpressed in the form

$$F=\alpha_1''P_1^2+\alpha_2''P_2^2+\alpha_{11}''(P_1^4+P_2^4)+\alpha_{12}''P_1^2P_2^2+\alpha_{111}(P_1^6+P_2^6)$$
$$+\alpha_{112}(P_1^2P_2^4+P_1^4P_2^2)+\frac{1}{2}g_{44}(P_{2,3}^2+P_{1,3}^2), \tag{7}$$

where α_1'' and α_2'' usually depends linearly on temperature, i.e., $\alpha_i'=\alpha_i^0+\alpha_0(T-T_0)$ with $\alpha_0>0$. Eventually, the variatonal derivative of the total free energy $\int F dx_3$ gives the equilibrium equations of the 180° wall as

$$g_{44}P_{1,33}=2\alpha_1''P_1+4\alpha_{11}''P_1^3+2\alpha_{12}''P_1P_2^2+6\alpha_{111}P_1^5$$
$$+2\alpha_{112}(P_1P_2^4+2P_1^3P_2^2), \tag{8a}$$

$$g_{44}P_{2,33}=2\alpha_2''P_2+4\alpha_{11}''P_2^3+2\alpha_{12}''P_1^2P_2+6\alpha_{111}P_2^5$$
$$+2\alpha_{112}(P_1^4P_2+2P_1^2P_2^3). \tag{8b}$$

It is evident that Eqs. (8a) and (8b) have the analytical solutions

$$P_1^I(x_3)=P_0\frac{\sinh(x/\delta^I)}{\sqrt{q^2+\cosh(x/\delta^I)}},\quad P_2^I(x_3)=0, \tag{9}$$

with $q^2=P_0^2/(2P_0^2-\alpha_{11}''/\alpha_{111})$ and

$$\delta^I=\sqrt{\frac{g_{44}}{3\alpha_{111}}}\ \frac{1}{P_0\sqrt{2P_0^2-3\alpha_{11}''/\alpha_{111}}}. \tag{10}$$

The solution for P_1^I is the kink-type solitary-wave solution, and the corresponding wall is often called an ''Ising-type'' (IT) wall (denoted by the superscript I) with its half width characterized by δ^I.[14] This kind of wall is usually considered to be the real structure of the 180° twin boundaries in ferroelectric perovskites.

However, numerical calculations show that, besides the IT solutions, Eqs. (8a) and (8b) have another set of solutions $P_1^B(x_3)$ and $P_2^B(x_3)$ which satisfy the boundary conditions of Eq. (5). This set of solutions can be solved by integrating Eqs. (8a) and (8b) from the wall center $x_3=0$ to $\pm\infty$. For this aim, we have to determine four initial values, $P_1^B(0)$, $P_2^B(0)$, $P_{1,3}^B(0)$, and $P_{2,3}^B(0)$. In view of Eq. (5), it is apparent that $P_1^B(0)=0$ and $P_{2,3}^B(0)=0$. The other two initial values, $P_2^B(0)$ and $P_{1,1}^B(0)$, are related by the first integral of Eqs. (8a) and (8b),

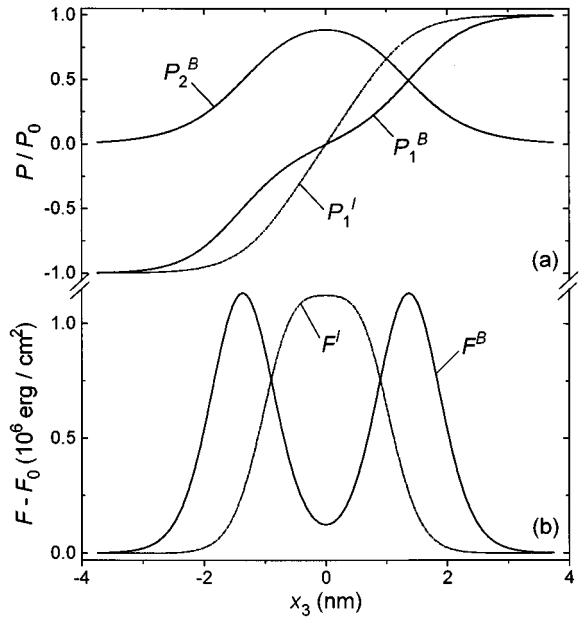

FIG. 1. Position dependence of spontaneous polarization and free energy density across IT and BT 180° walls for $BaTiO_3$ at $T=109$°C. (a) Polarization profiles. (b) Free energy density.

$$\frac{1}{2}g_{44}(P_{1,3}^2+P_{2,3}^2)=\alpha_1''P_1^2+\alpha_2''P_2^2+\alpha_{11}''(P_1^4+P_2^4)+\alpha_{12}''P_1^2P_2^2$$
$$+\alpha_{111}(P_1^6+P_2^6)+\alpha_{112}(P_1^2P_2^4+P_1^4P_2^2)$$
$$-F_0, \tag{11}$$

where $F_0=\alpha_1''P_0^2+\alpha_{11}''P_0^4+\alpha_{111}P_0^6$ is the free energy of the homogeneous state. So scanning only one nonzero initial value, say, $P_2^B(0)$ allows us to perform the integration and obtain the correct polariztion profiles $P_1^B(x_3)$ and $P_2^B(x_3)$ satisfying the boundary conditions. For instance, by substituting the parameters of $BaTiO_3$, $2\alpha_1''=2\alpha_2''=4\pi(T-T_0)/C$ ($C=1.7\times10^5$, $T_0=110$ °C), $4\alpha_{11}''=1.8\times10^{-14}(T-175)$, $2\alpha_{12}''=1.2\times10^{-12}$, $6\alpha_{111}=5.4\times10^{-22}$, and $2\alpha_{112}=8\times10^{-23}$ cgs,[12] into Eqs. (8a) and (8b), we obtain the space profiles of P_1^B and P_2^B as illustrated in Fig. 1(a). Here g_{44} has been reasonably chosen as 10^{-17} cm^2 and assumed to be temperature independent (its exact value can be calculated from the phonon dispersion curves.)[15] The wall associated with the solutions of P_1^B and P_2^B may be called a ''Bloch-type'' (BT) wall (denoted by the superscript B).[14] The microscopic structure of the BT wall is that the polarization vector $\mathbf{P}^B=P_1^B\hat{x}_1+P_2^B\hat{x}_2$ spirals from $-P_0\hat{x}_1$ to $P_0\hat{x}_1$ across the wall. This is different from the IT wall whose polarizaton vector keeps parallel to the x_1 axis. Moreover, it can be seen from Fig. 1(a) that the width of the BT wall is much greater than that of the IT wall.

Figure 1(b) shows the profiles of F^I and F^B corresponding to the IT and BT solutions in Fig. 1(a), respectively. Due to the occurrence of the polarization component P_2^B, F^B is significantly lower than F^I in the vicinty of the wall center. However, integration of F^I and F^B with respect to x_3 indicates that the total energy W^B of the BT wall is slightly higher than W^I of the IT wall. This implies that the BT wall

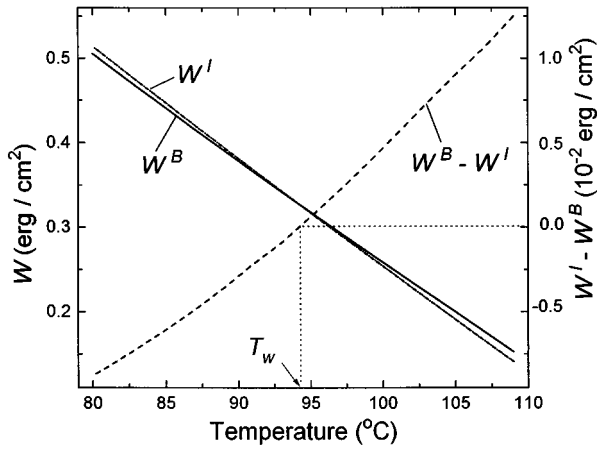

FIG. 2. Temperature dependence of interfacial energy of IT and BT walls in $BaTiO_3$. T_w is the temperature point where the two wall structures may change from one to the other.

is metastable while the IT wall is a stable structure in the temperature region close to T_0. It is known that domain wall energy usually increases when temperature decreases.[9] The temperature-dependent W^B and W^I calculated with the above parameters of $BaTiO_3$ are illustrated in Fig. 2. It is interesting that the increase of W^I is slightly more rapid than that of W^B, and there exists a temperature point $T_w = 94\,^\circ\mathrm{C}$ where the two walls have the same energy density. Below T_w, W^B is lower than W^I. From the energetical viewpoint, therefore, the 180° wall structure may change from IT to BT at the transformation point T_w upon cooling.

It can be seen that the solutions for both $\mathbf{P}^B$ and $\mathbf{P}^I$ are of quasione dimension and require some x_3-dependent stresses to clamp the walls so as to make them free of dislocation and disclinations. For the IT wall, the nonzero stresses are σ_{11} and σ_{22} while the BT wall needs an additional shear component σ_{12}. By taking into account the stressed state of the wall, the coefficients quoted in the above calculations may not be so accurate since most of them are for unstressed $BaTiO_3$. However, detailed calculations have shown that modification of the coefficients does not influence the main characteristics of the solutions of Eqs. (8a) and (8b). Moreover, the structural transformation between the IT and BT walls is a direct consequence of the temperature dependence of α_1'' and α_2'', as will be discussed below. Therefore, the results plotted in Figs. 1 and 2 represent the general features of the two kinds of 180° domain walls in the tetragonal phase of $BaTiO_3$.

The temperature dependence of the domain wall energy density implies that the BT wall can exist as a more stable structure in the wide low-temperature region. Thus the 180° walls found in $BaTiO_3$ at room temperature are actually BT interfaces. For this kind of wall as shown in Fig. 3, not only the magnitude of the polarization changes, the rotation of the polarization vector also occurs. The only x_3-dependent strain component is η_{33}^B which is related to the polarization components P_1^B and P_2^B by Eq. (6). The x_3-dependent stresses required to keep the strains η_{11}, η_{22}, and $\eta_{12}\,(=0)$ constant across the BT wall are

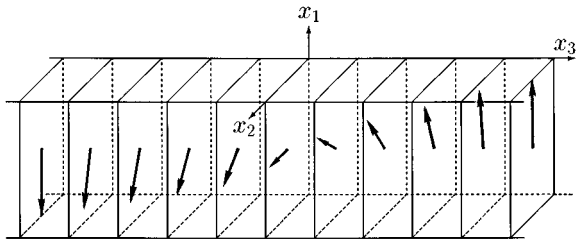

FIG. 3. Schematic representation of the BT wall. All the arrows lie within the x_1x_2 plane and indicate the polarization vector $\mathbf{P}^B$; the lattice constants along x_1 and x_2 keep constant; the wall has no shear deformation, but the structure is monoclinic due to the inclination of the polarization from x_1.

$$\sigma_{11}^B = C_{11}Q_{11}P_0^2 - q_{11}P_1^{B2} - q_{12}P_2^{B2},$$

$$\sigma_{22}^B = C_{11}Q_{12}P_0^2 - q_{11}P_2^{B2} - q_{12}P_1^{B2},$$

$$\sigma_{12}^B = -2q_{44}P_1^BP_2^B, \tag{12}$$

respectively, and usually these stresses are provided automatically by the domains sandwiching the wall to resist the tendency of ''lattice mismatching'' in the vicinty of the wall. Based on the fact that no shear deformation occurs within the wall layer, the crystal symmetry seems to be orthorhombic. But if we note that the coexistence of P_1^B and P_2^B results from the ionic displacement along both x_1 and x_2 directions, the BT wall structure is in fact monoclinic. Subsequently, the monoclinic structure makes the BT wall birefringent along the x_1 axis. Experiments have shown that, indeed, the 180° walls in $BaTiO_3$ are directly visible between crossed polarizers even with no external electric field normal to the polar axis applied.[16] This effect is a unique property of ferroelectric perovskites, and it proves the existence of 180° BT walls in $BaTiO_3$ at room temperature.

The IT wall also has a position-dependent strain component η_{33}^I but the crystal symmetry is strictly orthorhombic (or quasitetragonal) since the polarization vector is always parallel to x_1. Generally speaking, the orthorhombic structure is also birefringent. In the case of the IT wall structure, however, the birefringence arising from the slight variation of the interplanar spacing along the normal of the wall is believed to be negligible, similar to the 180° walls of uniaxial ferroelectrics (e.g., $LiNbO_3$) which are invisible under polarized light. On the other hand, the limited resolution of the polarizing microscopy may also be attributable to the invisibility of the IT walls even if they are birefringent, because the thickness of the IT wall layer is much smaller than that of the BT wall.

It is worth noting the physical origin of the IT-BT transformation of the wall structures at low temperature. In view of the free energy, the decreases of the negative coefficients α_i' (as well as α_{11}'') in Eq. (7) below T_0 make the spontaneous polarization larger and, particularly, give rise to more polarization components. It is this effect that leads to the cubic-tetragonal-orthorhombic-rhombohedral phase transitions of perovskites upon cooling with the polarization increasing from one component to two and then to three in turn. However, since the wall has a special structure distorted from the tetragonal lattice, the temperature at which the one-

component polarization transforms into the two-component one is, expectedly, different from the tetragonal-orthorhombic transition temperature $T_{\text{T-O}}$ of the homogeneous crystal [in the present case of $BaTiO_3$, T_w is much higher than $T_{\text{T-O}}$ ($\simeq 0\,^\circ\text{C}$)]. Consequently, the excess energy W^B of the two-component wall is lower than W^I of the one-component wall. On the other hand, the IT-BT transformation can significantly decrease the free energy density at the wall center. In Fig. 1(b), we have seen that $F^B(0)$ is much smaller than $F^I(0)$. Calculations have shown that, below T_w, the two peaks of F^B besides the wall center disappear while $F^B(0)$ stays smaller than $F^I(0)$. This means that the F^B curve is more flat and wider than F^I. Therefore, the BT wall is an energetically stable structure in the low temperature range with the excess energy distributed in a wide region. Furthermore, the switching of antiparallel domains is often realized by the nucleation and growth of new domains. During the motion of the IT wall toward $+x_3$ direction (see Fig. 1), the polarization first decreases from P_0 to zero, and then changes to $-P_0$. This process often requires the domain to surmount a high potential barrier. For the movement of the BT wall, the polarization vector is *rotated* from P_0 to $-P_0$, and its magnitude keeps nonzero throughout the reversal process. In this case, the potential barrier is relatively low, indicating that the BT wall is more mobile than the IT wall. From the consideration of domain kinetics, the preferable structure of the 180° wall is also of Bloch type.

Up to now we have completely ignored the thermal fluctuations of the order parameters which are known to have possibly dramatic effects on mean-field results at temperature close to the transition point. However, the Landau-Ginzburg theory is valid as long as the fluctuations in a volume with linear dimensions of the order of the correlation length are small compared with the equilibrium order parameter P_0,[17] and this condition is generally satisfied in the temperature range away from the transition temperature. For the above results obtained from such a temperature range, the influence of fluctuations is believed to be negligible.

In conclusion, we have demonstrated that the 180° domain walls in tetragonal phase of $BaTiO_3$ can take two kinds of structures, one of Bloch type and the other of Ising type, in different temperature regions, and the structural transformation of the walls from the former to the later upon cooling originates directly from the decrease of α_i' which has a tendency to give rise to more polarization components in perovskites. Since our results are obtained from the general pheneomenology of the first-order O_h-C_{4v} ferroelectric phase transition and the main characteristics of the results are independent of the parameters used in the calculations, the existence of two 180° twinning structures and the associated wall transformation are common features for all ferroelectric perovskites. Moreover, it can be proved that, as long as the Landau-Ginzburg theory is valid, other kinds of electrically neutral twin boundaries, such as 90°, 120°, and 60° walls, in all the ferroelectric phases (including tetragonal, orthorhombic, and rhombohedral phases) of perovskites have the same equilibrium equations as Eqs. (8a) and (8b), only that the expansion coefficients or boundary conditions are different. For these walls, the IT-like kink solutions always exist, but the BT-like polarization configuration may also be obtainable within certain temperature region. If the expansion coefficients (as well as their temperature dependence) in the free-energy equation (1) are determined experimentally, one can apply the present model to obtain the detailed structures of these walls.

This work was supported by the National Natural Science Foundation of China, National Laboratory of BEPC, and Institute of Crystal Materials, Shandong University.

[1] M. E. Lines and A. M. Glass, *Principles and Applications of Ferroelectrics and Related Materials* (Clarendon, Oxford, 1977), p. 87.
[2] C. Boulesteix, Phys. Status Solidi A **86**, 11 (1984); R. Spycher, P. A. Buffat, and P. Stadelmann, Helv. Phys. Acta **60**, 804 (1987); F. Tsai and J. M. Cowley, Ferroelectrics **140**, 203 (1993); X. Zhang, T. Hashimoto, and D. C. Joy, Appl. Phys. Lett. **60**, 784 (1992).
[3] V. A. Zhirnov, Sov. Phys. JETP **35**, 822 (1959).
[4] A. Gordon, Physica **122B**, 321 (1983).
[5] J. Lajzerowicz, Ferroelectrics **35**, 219 (1981).
[6] W. Cao and G. R. Barsch, Phys. Rev. B **41**, 4334 (1990).
[7] A. Amin, M. J. Haun, B. Badger, H. McKinstry, and L. E. Cross, Ferroelectrics **65**, 107 (1985).
[8] Wenwu Cao and L. E. Cross, Phys. Rev. B **44**, 5 (1991).
[9] X. R. Huang, S. S. Jiang, X. B. Hu, X. Y. Xu, W. Zeng, D. Feng, and J. Y. Wang, Phys. Rev. B **52**, 9932 (1995).
[10] S. R. Andrews and R. A. Cowley, J. Phys. C **19**, 615 (1986).
[11] M. Rober, I. Reaney, and P. Stadelmann, Physica A **229**, 47 (1996); Helv. Phys. Acta **66**, 55 (1993).
[12] T. Mitsui, I. Tatsuzaki, and E. Nakamura, *An Introduction to the Physics of Ferroelectrics* (Gordon and Breach, New York, 1976), p. 142.
[13] J. R. Barber, *Elasticity* (Kluwer Academic Publishers, Dordrecht, 1992), p. 22.
[14] J. Lajzerowicz and B. Houchmandzadeh, Ferroelectrics **140**, 81 (1993).
[15] Wenwu Cao, J. Phys. Soc. Jpn. **63**, 1156 (1994).
[16] J. Kobayashi and N. Yamada, Phys. Rev. Lett. **11**, 410 (1963).
[17] A. Z. Patashinskiĭ and V. L. Pokrovskiĭ, *Fluctuation Theory of Phase Transitions* (Pergamon Press, Oxford, 1979).